2009 International Nuclear Atlantic Conference - INAC 2009
Rio de Janeiro,RJ, Brazil, September27 to October 2, 2009
ASSOCIAÇÃO BRASILEIRA DE ENERGIA NUCLEAR - ABEN
ISBN: 978-85-99141-03-8

An Analytical Spatial Reconstruction Algorithm for the SD-SGF-CN Hybrid Nodal Method for One-Speed X,Y-Geometry S_N Eigenvalue Problems

Welton Alves Menezes, Hermes Alves Filho and Ricardo C. Barros

Departamento de Modelagem Computacional
Instituto Politécnico
Universidade do Estado do Rio de Janeiro
Rua Alberto Rangel s/n 28630-050 Nova Friburgo, RJ, Brasil
walves@iprj.uerj.br
halves@iprj.uerj.br
rcbarros@pq.cnpq.br

ABSTRACT

In this paper the X,Y-geometry SD-SGF-CN spectral nodal method, *cf.* spectral diamond-spectral Green's function-constant nodal, is used to determine the one-speed node-edge average angular fluxes in heterogeneous domains. This hybrid spectral nodal method uses the spectral diamond (SD) auxiliary equation for the multiplying regions and the spectral Green's function (SGF) auxiliary equation for the non-multiplying regions of the domain. Moreover, we consider constant approximations for the transverse-leakage terms in the transverse integrated S_N nodal equations. We solve the SD-SGF-CN equations using the one-node block inversion (NBI) iterative scheme, which uses the most recent estimates available for the node-entering fluxes to evaluate the node-exiting fluxes in the directions that constitute the incoming fluxes for the adjacent node. Using these results, we offer an algorithm for analytical reconstruction of the coarse-mesh nodal solution within each spatial node, as localized numerical solutions are not generated by usual accurate nodal methods. Numerical results are presented to illustrate the accuracy of the present algorithm.

Keywords: neutron transport equation, discrete ordinates, nodal methods, eigenvalue problems.

1. INTRODUCTION

Neutral particle transport mathematical modeling is generally performed using the linearized Boltzmann equation because of its similarity with the expression obtained by L. Boltzmann in connection with kinetic theory of gases [1]. This is a linear integro-differential equation, where particles are considered to interact with matter without affecting its structure and interacting with each other. The neutron transport equation represents a balance between gains and loss of particles, and generally depends on seven independent variables: three on space, two on direction of motion, one depends on energy, and one on time.

A simple, though efficient form to treat the angular variable that indicates the particle direction of motion is to discretize these variables using the discrete ordinates method, also termed as S_N method [2; 3; 4]. This formulation is one of the most traditional approximations

in neutron transport theory. The S_N formulation in based on the discretization of the angular variables, taking the transport equation in a discrete set of directions (discrete ordinates). The angular integrals that appear in the source terms are numerically approximated by quadrature formulas.

In this work we use the S_N "Spectral Diamond-Spectral Green's Function-Constant Nodal (SD-SGF-CN) method for one-speed X,Y-geometry model. This coarse-mesh method is based on the use of standard spatially discretized S_N balance equations [5] and two types of auxiliary equations that preserve the nodal general solutions. In the non-multiplying regions, e.g., the reflector, we use the spectral Green's function (SGF) auxiliary equations. In the multiplying regions, e.g., the fuel assemblies, we use the spectral diamond (SD) auxiliary equations. Moreover, we consider constant approximations for the transverse-leakage terms in the transverse integrated S_N nodal equations. This hybrid characteristic of the SD-SGF method improves both the numerical stability and the convergence rate of the inner iterations in coarse-mesh calculations. In the inner iterations we use the non-conventional NBI iterative scheme, *cf.* the "one-node block inversion", and in the outer iterations we use the power method [6].

The main advantage of the use of nodal methods, in particular the SD-SGF-CN method, is the reduction of the number of points in the discretized equations. This generally implies sharp reduction in execution time and allocation of computer memory compared with traditional fine-mesh methods applied to transport problems [5; 7; 8]. In contrast to the gain in efficiency of coarse-mesh methods, detailed information in the profile of the numerical solution are not provided. To go around this drawback, we use the coarse-mesh numerical solution as generated by the SD-SGF-CN method, to derive an algorithm for the reconstruction of within node dominant solution.

An outline of the remainder of this paper follows. In section 2, we describe the within node analytical reconstruction scheme we offer in this paper. In section 3, we show numerical results to a typical model problem and a number of concluding remarks are given in section 4.

2. THE WITHIN NODE ANALYTICAL RECONSTRUCTION SCHEME

2.1 Analytical Spatial Reconstruction Scheme

Let us consider an arbitrary spatial grid $\Gamma_x \times \Gamma_y$ defined on a rectangular domain D of length L and height H as shown in Figure 1. The spatial grid is composed of $I \times J$ spatial nodes $D_{i,j}$ of length h_{xi} and height h_{yj}.

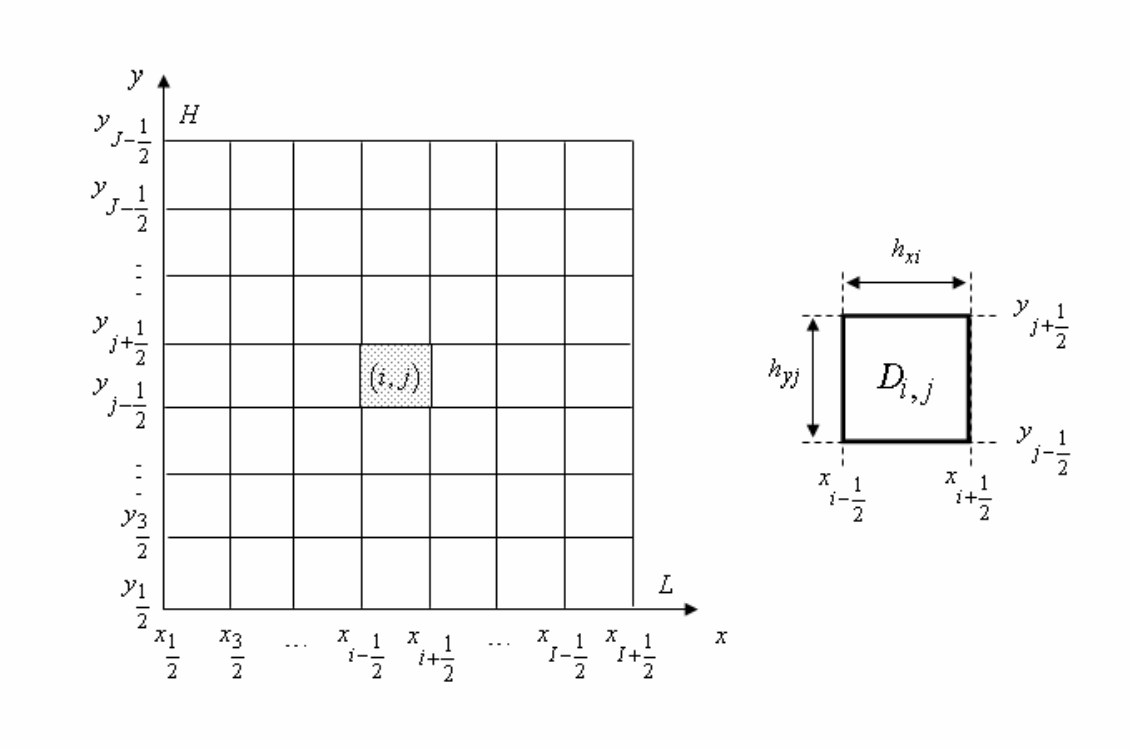

Figure 1. Spatial Grid $\Gamma_x \times \Gamma_y$

Now we consider the discrete ordinates (S_N) equations with isotropic scattering defined in an arbitrary node $D_{i,j}$.

$$\left[\mu_m \frac{\partial}{\partial x} + \eta_m \frac{\partial}{\partial y} + \sigma_T(x,y)\right]\psi_m(x,y) = \frac{\sigma_S(x,y)}{4}\sum_{n=1}^{M}\psi_n(x,y)\omega_n + \frac{\nu\sigma_f(x,y)}{4k_{eff}}\sum_{n=1}^{M}\psi_n(x,y)\omega_n \quad , \tag{1}$$

$(x,y) \in \Gamma_x \times \Gamma_y \quad , \quad m = 1:M.$

Here the notation is standard and we use the level symmetric quadrature set [5].
Integrating Eq.(1) over the spatial directions y and x on the sides of the nodes $D_{i,j}$ and considering constant approximations for the transverse-leakage terms, we obtain the S_N transverse-integrated nodal equations

$$\mu_m \frac{d}{dx}\tilde{\psi}_{m,j}(x) + \sigma_{Ti,j}\tilde{\psi}_{m,j}(x) = \frac{\sigma_{i,j}(k_{eff})}{4}\sum_{n=1}^{M}\tilde{\psi}_{n,j}(x)\omega_n - \frac{\eta_m}{h_{yj}}\left[\hat{\psi}_{m,i,j+½} - \hat{\psi}_{m,i,j-½}\right] \quad , \tag{2}$$

$$\eta_m \frac{d}{dy}\hat{\psi}_{m,i}(y) + \sigma_{Ti,j}\hat{\psi}_{m,i}(y) = \frac{\sigma_{i,j}(k_{eff})}{4}\sum_{n=1}^{M}\hat{\psi}_{n,i}(y)\omega_n - \frac{\mu_m}{h_{xi}}\left[\tilde{\psi}_{m,i+½,j} - \tilde{\psi}_{m,i-½,j}\right] \quad ,$$

$m = 1:M$, (3)

where we have defined the node-edge average angular flux

$$\tilde{\psi}_{m,j}(x) \equiv \frac{1}{h_{yj}}\int_{y_{j-½}}^{y_{j+½}}\psi_m(x,y)dy \quad , \tag{4}$$

$$\hat{\psi}_{m,i}(y) \equiv \frac{1}{h_{xi}} \int_{y_{i-1/2}}^{y_{i+1/2}} \psi_m(x,y)dx \quad . \tag{5}$$

The expressions of the general solutions of Eqs.(2-3) can be written respectively by

$$\tilde{\psi}_{m,j}(x) = \tilde{\psi}^P_{m,i,j} + \tilde{\psi}^H_{m,j}(x) \quad , \tag{6}$$

$$\hat{\psi}_{m,i}(y) = \hat{\psi}^P_{m,i,j} + \hat{\psi}^H_{m,i}(y) \quad , \tag{7}$$

where the superscript P denotes the particular solution and the superscript H the homogeneous solution. A more detailed description of how we have calculated the particular solution and homogeneous solution is provided in Ref. [10-12].

A limitation of coarse-mesh methods, e.g., spectral-nodal methods, is the generation of neutron-flux profile in specific points inside the spatial nodes. Though precise, these methods do not provide detailed information in neutron flux profile. Traditionally, this information is obtained using the computationally expensive fine-mesh methods. An efficient alternative is to use a nodal method to generate angular fluxes at the node edges and with these results make a within-node reconstruction [9; 10]. To reconstruct the neutron scalar flux inside an arbitrary node $D_{i,j}$, we must evaluate expression

$$\phi_k(u) = \frac{1}{4} \sum_{n=1}^{M} \psi_{n,k}(u)\omega_n \quad , \tag{8}$$

where $k = i$ (or j), $u = y$ (or x), and $u \in \left\lfloor u_{l-1/2}; u_{l+1/2} \right\rfloor$, whit $l = j$ (or i). Therefore, if $k = i \Rightarrow u = y \Rightarrow l = j$, consequently

$$\phi_k(u) = \hat{\phi}_i(y) = \frac{1}{4} \sum_{n=1}^{M} \hat{\psi}_{n,i}(y)\omega_n \quad , \quad y \in \left[y_{j+1/2}; y_{j-1/2} \right] \quad . \tag{9}$$

A similar result is obtained for $k = j$.

The starting point for the analytical reconstruction scheme is the definition of the complex kernel of the local S_N operator. Let us denote the complex kernel by

$$K_j \equiv [\psi(u) \ / \ T_j\psi(u) \ = \ 0 \ , \ u \ \in \ \Gamma_{i,j}] \ , \tag{10}$$

where T_j is the local S_N operator and the square brackets indicate the linear space spaned by $\psi(u)$. After a spectral analysis of the transverse-integrated S_N equations, we can determine a basis for the complex M-dimensional linear space. This set of M linearly independent functions can be expressed by

$$B_j \equiv [\psi_l(u) \ / \ T_j\psi_l(u) \ = \ 0 \ , \ u \ \in \ \Gamma_i \times \Gamma_j \ , \ l \ = \ 1:M] \ , \tag{11}$$

where $\psi_l(u)$ is an element of a basis of K_j given by

$$\psi_l(u) \equiv [\psi_{1,1,\nu_l}(u)\ \ \psi_{1,2,\nu_l}(u)\ \ \ldots\ \ \psi_{2,1,\nu_l}(u)\ \ \psi_{2,2,\nu_l}(u)\ \ \ldots\ \ \psi_{M,k,\nu_l}(u)\ ]^T\ , \qquad (12)$$

where we have defined

$$\psi_{m,k,\nu_l}(u)\ =\ \psi_{m,k}(u,\nu_l)\ ,\ m,l\ =\ 1:M\ , \qquad (13)$$

and $\psi_{m,k,\nu_l}(u)$ is considered to determine the analytical solution of the homogeneous S_N transverse-integrated equations, with eigenvalues ν belonging to the spectrum of the S_N operator.

Considering these definitions, the general analytical solution of the S_N transverse-integrated nodal equations appears as

$$\psi_{m,k}(u)\ =\ \psi^{p,u}_{m,k,k'}\ +\sum(\alpha^u_l + i\beta^u_l)a^u_m(\nu_l)\exp(-\frac{\sigma_{Ti,j}u}{\nu_l})\ ,\ m=1:M\ . \qquad (14)$$

The offered scheme aims to determine the coefficients $(\alpha^u_l + i\beta^u_l)$ in Eq.(14). These coefficients are unique solution of a system of M linear equations, which is obtained from Eq.(14). This analysis is based on the nature of the S_N spectrum, which leads to a matrix of order M associated with a system of M linear equations. Therefore, we refer to this matrix as the local matrix for reconstruction.

To obtain the matrices for local reconstruction and the right-hand side vectors, we review the field of complex numbers of Eq.(14). Considering the real and imaginary parts of Eq.(14), we write

$$\psi'_{m,k}(u)\ =\sum_{l=1}^{M}(\alpha^u_l + i\beta^u_l)[\Re e\ \psi_{m,k,\nu_l}(u)\ +\ \Im m\ \psi_{m,k,\nu_l}(u)],\ m=1:M\ . \qquad (15)$$

where $\Re e\ \psi_{m,k,\nu_l}(u)$ e $\Im m\ \psi_{m,k,\nu_l}(u)$ are defined as the real and imaginary parts of the expression of $\psi_{m,k,\nu_l}(u)$ and define

$$\psi'_{m,k}(u)\ =\psi_{m,k}(u)\ -\ \psi^{p,u}_{m,k,k'}(u),\ m=1:M\ . \qquad (16)$$

After some algebra in Eq.(14), we obtain

$$\begin{aligned}\psi'_{m,k}(u)\ =&\sum_{l=1}^{M}\{[\alpha^u_l\Re e\ \psi_{m,k,\nu_l}(u)-\beta^u_l\Im m\ \psi_{m,k,\nu_l}(u)]\\ &+\ i[\beta^u_l\Re e\ \psi_{m,k,\nu_l}(u)\ +\ \alpha^u_l\Im m\ \psi_{m,k,\nu_l}(u)]\},\ m=1:M\ .\end{aligned} \qquad (17)$$

Equation (17) is the starting point for the analysis we describe. To illustrate, let us consider the two types of spectra:

1. Real spectrum

For this type of spectrum, the imaginary part of eigenfunctions $\psi_{m,k,\nu_l}(u)$ is equal to zero and hence Eq.(17) is given by

$$\psi'_{m,k}(u) = \sum_{l=1}^{M} \{[\alpha_l^u \Re e\ \psi_{m,k,\nu_l}(u) - \beta_l^u \Im m\ \psi_{m,k,\nu_l}(u)]\ ,\ m = 1:M\ . \tag{18}$$

Since the dominant solution is a real function, we write

$$\sum_{l=1}^{M} \beta_l^u \psi_{m,k,\nu_l}(u) = 0\ ,\ m = 1:M\ . \tag{19}$$

Since these eigenfunctions constitute a linearly independent set in K_j, the constants β_l^u are equal to zero for all l. Therefore, Eq.(18) appears as

$$\psi'_{m,k}(u) = \sum_{l=1}^{M} \alpha_l^u \Re e\ \psi_{m,k,\nu_l}(u)\ ,\ m = 1:M\ . \tag{20}$$

Equation (20) can be identified as a system of M linear equations in M unknowns α_l^u. Each system has coefficients given by the values of the eigenfunctions $\psi_{m,k,\nu_l}(u)$ and the right-hand side vector is given by the numerical solution for $\psi'_{m,k}(u)$ generated by the SD-SGF-CN coarse-mesh nodal method at the region edges for reconstruction. The system for the α_l^u in matrix form appears as

$$\begin{bmatrix} \psi_{1Q,\nu_1}^{k-1/2} & \psi_{1Q,\nu_2}^{k-1/2} & \cdots & \psi_{1Q,\nu_M}^{k-1/2} \\ \psi_{4Q,\nu_1}^{k-1/2} & \psi_{3Q,\nu_2}^{k-1/2} & \cdots & \psi_{4Q,\nu_M}^{k-1/2} \\ \psi_{2Q,\nu_1}^{k+1/2} & \psi_{1Q,\nu_2}^{k+1/2} & \cdots & \psi_{2Q,\nu_M}^{k+1/2} \\ \psi_{3Q,\nu_1}^{k+1/2} & \psi_{3Q,\nu_2}^{k+1/2} & \cdots & \psi_{3Q,\nu_M}^{k+1/2} \end{bmatrix} \begin{bmatrix} \alpha_{1Q}^u \\ \alpha_{4Q}^u \\ \alpha_{2Q}^u \\ \alpha_{3Q}^u \end{bmatrix} = \begin{bmatrix} \psi_{1Q}^{'k-1/2} \\ \psi_{4Q}^{'k-1/2} \\ \psi_{2Q}^{'k+1/2} \\ \psi_{3Q}^{'k+1/2} \end{bmatrix}, \tag{21}$$

where $\psi_{m,\nu_1}^{k-1/2}$ and $\psi_{m,\nu_1}^{k+1/2}$ are the values of the eigenfunctions $\psi_{m,\nu_l}(u)$ at the region edges in one fixed spatial direction x or y. The right-hand side vector of Eq. (21) corresponds to the coarse-mesh numerical solutions generated by the SD-SGF-CN code. We remark that the subscript 1Q is defined as the first quadrant of the Cartesian coordinate system and an element of the first row of the coefficient matrix for the particular case of N = 4 and hence M = 12, is expressed by

$$\psi_{1Q,\nu_1}^{k-1/2} = [\psi_{1,\nu_1}^{k-1/2}\ \psi_{2,\nu_1}^{k-1/2}\ \psi_{3,\nu_1}^{k-1/2}\ ]^T. \tag{22}$$

The system (21) is solved for the coefficients α_l^u and so a complete description of the dominant analytical solution $\psi_m(u)$ in $\Gamma_{i,j}$ is obtained.

2. Spectrum consists of a pair of purely imaginary eigenvalues and $\frac{N-2}{2}$ pairs of real eigenvalues

For simplicity, we order the eigenvalues such that the first 2 eigenvalues correspond to the pair of purely imaginary eigenvalues. Therefore, Eq. (17) is expressed by

$$\begin{aligned}\psi'_{m,k}(u) &= \sum_{l=1}^{2}\{[\alpha_l^u \Re e\ \psi_{m,k,\nu_l}(u) - \beta_l^u \Im m\ \psi_{m,k,\nu_l}(u)] \\ &\quad + i[\beta_l^u \Re e\ \psi_{m,k,\nu_l}(u) + \alpha_l^u \Im m\ \psi_{m,k,\nu_l}(u)]\} \\ &\quad + \sum_{l=3}^{M}[\alpha_l^u \psi_{m,k,\nu_l}(u) + i\beta_l^u \psi_{m,k,\nu_l}(u)]\ ,\end{aligned} \tag{23}$$

where $\Im m\ \psi_{m,k,\lambda_l i}(u) = 0$ for $l = 3:M$.

The S_N spectrum has the property that $\psi_{m,k,\lambda_l i}(u)$ is complex conjugate of $\psi_{m,k,-\lambda_l i}(u)$, i.e.,

$$\Re e\ \psi_{m,k,\lambda_l i}(u) = \Re e\ \psi_{m,k,-\lambda_l i}(u)\ , \tag{24}$$

and

$$\Im m\ \psi_{m,k,\lambda_l i}(u) = -\Im m\ \psi_{m,k,-\lambda_l i}(u)\ . \tag{25}$$

By substituting these results into Eq.(23), we obtain

$$\begin{aligned}\psi'_{m,k}(u) &= [(\alpha_1^u + \alpha_2^u)\Re e\ \psi_{m,k,\nu_l}(u) + (\beta_1^u - \beta_2^u)\Im m\ \psi_{m,k,\nu_l}(u)] \\ &\quad + i[(\beta_1^u + \beta_2^u)\Re e\ \psi_{m,k,\nu_l}(u) + (\alpha_1^u - \alpha_2^u)\Im m\ \psi_{m,k,\nu_l}(u)] \\ &\quad + \sum_{l=3}^{M}[\alpha_l^u \psi_{m,k,\nu_l}(u) + i\beta_l^u \psi_{m,k,\nu_l}(u)]\ .\end{aligned} \tag{26}$$

Considering the real and imaginary parts of Eq (26), we obtain

$$\begin{aligned}\Re e\ \psi_{m,k,\nu_l}(u) &= [(\alpha_1^u + \alpha_2^u)\Re e\ \psi_{m,k,\nu_l}(u) + (\beta_1^u - \beta_2^u)\Im m\ \psi_{m,k,\nu_l}(u)] \\ &\quad + \sum_{l=3}^{M}\alpha_l^u \psi_{m,k,\nu_l}(u)\ ,\end{aligned} \tag{27}$$

and

$$\Im m\ \psi_{m,k,\nu_l}(u) \;=\; (\beta_1^u+\beta_2^u)\Re e\ \psi_{m,k,\nu_l}(u) \;+\; (\alpha_1^u-\alpha_2^u)\Im m\ \psi_{m,k,\nu_l}(u) + \sum_{l=3}^{M}\beta_l^u\psi_{m,k,\nu_l}(u)\ . \tag{28}$$

Following the same reasons we set to derive Eqs. (18) and (19), we obtain from Eq. (28) the following results:

$$i)\ \ \beta_1^u=-\beta_2^u \text{ and } \alpha_2^u=\alpha_1^u\ ,$$
$$and$$
$$ii)\ \ \beta_1^u=0 \text{ for } l=3:M$$

Substituting these results into Eq (27) and identifying $\Re e\ \psi'_{m,k}(u)=\psi'_{m,k}(u)$, the general solution of the transverse integrated S_N equations in $\Gamma_{i,j}$ can be expressed by

$$\psi'_{m,k}(u) \;=[(\alpha_1^u 2\Re e\ \psi_{m,k,\nu_l}(u)-\beta_1^u 2\Im m\ \psi_{m,k,\nu_l}(u)] + \sum_{l=3}^{M}\alpha_l^u\psi_{m,k,\nu_l}(u)\ ,\ \ m=1:M\ . \tag{29}$$

Similarly to the case (1) (real spectrum), Eq (29) is also identified with a system of M linear equations in M unknowns. In analogy to the case of real spectrum, the system for the local reconstruction scheme in matrix notation appears as

$$\begin{bmatrix} 2\Re e\ \psi_{1Q,\nu_1}^{k-1/2} & -2\Im m\ \psi_{1Q,\nu_2}^{k-1/2} & \cdots & \psi_{1Q,\nu_M}^{k-1/2} \\ 2\Re e\ \psi_{4Q,\nu_1}^{k-1/2} & -2\Im m\ \psi_{3Q,\nu_2}^{k-1/2} & \cdots & \psi_{4Q,\nu_M}^{k-1/2} \\ 2\Re e\ \psi_{2Q,\nu_1}^{k+1/2} & -2\Im m\ \psi_{1Q,\nu_2}^{k+1/2} & \cdots & \psi_{2Q,\nu_M}^{k+1/2} \\ 2\Re e\ \psi_{3Q,\nu_1}^{k+1/2} & -2\Im m\ \psi_{3Q,\nu_2}^{k+1/2} & \cdots & \psi_{3Q,\nu_M}^{k+1/2} \end{bmatrix} \begin{bmatrix} \alpha_{1Q}^u \\ \alpha_{4Q}^u \\ \alpha_{2Q}^u \\ \alpha_{3Q}^u \end{bmatrix} = \begin{bmatrix} \psi'^{k-1/2}_{1Q} \\ \psi'^{k-1/2}_{4Q} \\ \psi'^{k+1/2}_{2Q} \\ \psi'^{k+1/2}_{3Q} \end{bmatrix}\ . \tag{30}$$

Once we have obtained the coefficients α_1^u, β_1^u and α_l^u, $l=3:M$, we can obtain a complete description of the dominant analytical solution $\psi_m(u)$ inside $\Gamma_{i,j}$.

3. NUMERICAL RESULTS

Let us consider a heterogeneous model problem as illustarted in Figure 2. The dimensions of the regions are represented in cm. We solve this problem using the SD-SGF-CN method, with standard S_4 level symmetric quadrature set [5] and the NBI [11] iterative scheme. Table

1 displays the material data for the four regions. Dimensions of all macroscopic cross sections are in cm^{-1}.

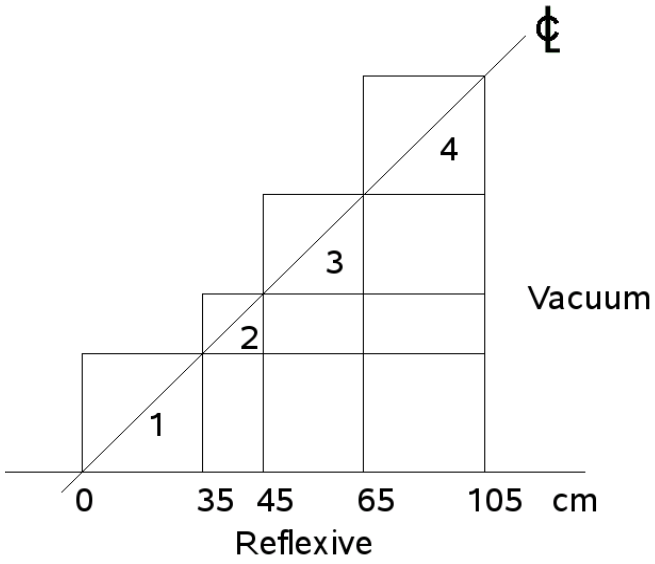

Figure 2. Model Problem

Table 1. Material Data for Model Problem

Material zone	σ_T (cm^{-1})	σ_S (cm^{-1})	$\nu\sigma_f$ (cm^{-1})
1[a]	$2.22589\ 10^{-1}$	$2.20563\ 10^{-1}$	$2.83283\ 10^{-3}$
2	$2.16566\ 10^{-1}$	$2.10697\ 10^{-1}$	$1.04347\ 10^{-2}$
3	$3.01439\ 10^{-1}$	$2.96069\ 10^{-1}$	$5.13036\ 10^{-4}$
4	$2.52250\ 10^{-1}$	$2.50794\ 10^{-1}$	$0.000000\ 10^{0}$

[a] see Figure 2.

In Table 2 and Figure 3, 4, 5 and 6 we present, respectively, the results and profiles of the node-edge average scalar fluxes generated by the present analytical within-node reconstruction scheme using the SD-SGF-CN method.

Table 2. Numerical results to the model problem

Region	Position (cm) x or y [b]	Method SD-SGF-CN	$\tilde{\phi}(x)$ or $\hat{\phi}(y)$	$\delta(\%)$ [c]
1[a]	0.00	$2.255460\ 10^{3}$	$2.254297\ 10^{3}$	$5.156\ 10^{-2}$
	8.75	$2.226970\ 10^{3}$	$2.223015\ 10^{3}$	$1.776\ 10^{-1}$
	17.50	$2.142742\ 10^{3}$	$2.138869\ 10^{3}$	$1.807\ 10^{-1}$
	26.50	$2.006981\ 10^{3}$	$2.005722\ 10^{3}$	$6.273\ 10^{-2}$
	35.0	$1.841218\ 10^{3}$	$1.841143\ 10^{3}$	$4.073\ 10^{-3}$
2	0.00	$1.324744\ 10^{3}$	$1.326745\ 10^{3}$	$1.510\ 10^{-1}$
	2.50	$1.245414\ 10^{3}$	$1.248892\ 10^{3}$	$2.793\ 10^{-1}$
	5.00	$1.154860\ 10^{3}$	$1.154092\ 10^{3}$	$6.650\ 10^{-2}$
	7.50	$1.049993\ 10^{3}$	$1.045522\ 10^{3}$	$4.258\ 10^{-1}$
	10.0	$9.277839\ 10^{2}$	$9.241963\ 10^{2}$	$3.867\ 10^{-1}$
3	0.00	$4.139151\ 10^{2}$	$4.109378\ 10^{2}$	$7.193\ 10^{-1}$
	5.00	$3.308628\ 10^{2}$	$3.242977\ 10^{2}$	$1.984\ 10^{0}$
	10.00	$2.618006\ 10^{2}$	$2.618206\ 10^{2}$	$7.639\ 10^{-3}$
	15.00	$2.168007\ 10^{2}$	$2.132401\ 10^{2}$	$1.642\ 10^{0}$
	20.00	$1.693592\ 10^{2}$	$1.723553\ 10^{2}$	$1.769\ 10^{0}$
4	0.00	$6.654450\ 10^{1}$	$6.626833\ 10^{1}$	$4.150\ 10^{-1}$
	10.00	$4.788566\ 10^{1}$	$4.711360\ 10^{1}$	$1.612\ 10^{0}$
	20.00	$3.156315\ 10^{1}$	$3.158615\ 10^{1}$	$7.287\ 10^{-2}$
	30.00	$1.706555\ 10^{1}$	$1.774016\ 10^{1}$	$3.953\ 10^{0}$
	40.00	$3.068705\ 10^{0}$	$3.347281\ 10^{0}$	$9.078\ 10^{0}$

[a] see Figure 2.

[b] 4 spatial nodes in the direction x and 4 spatial nodes in the direction y.

[c] relative deviation.

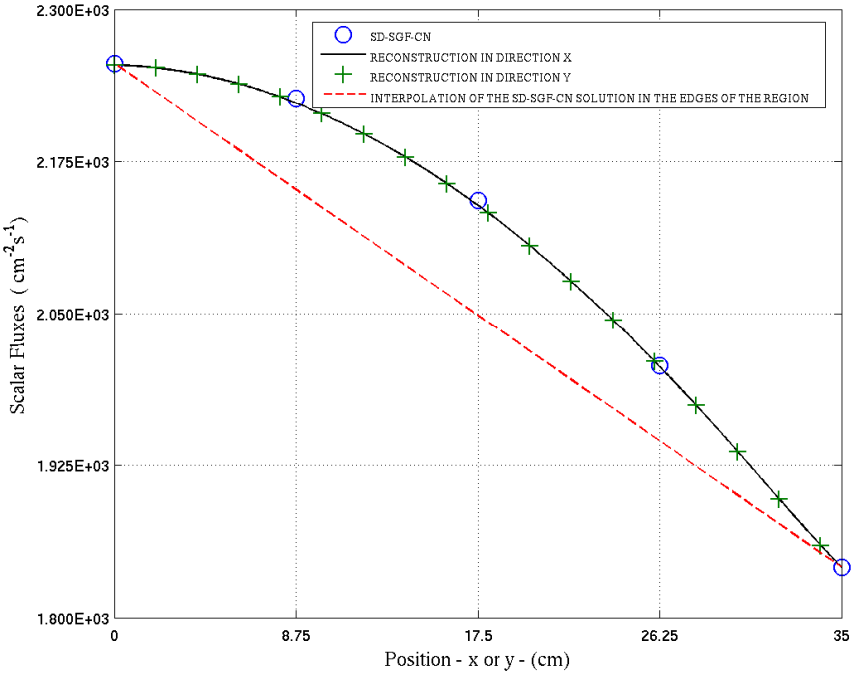

Figure 3. Scalar Flux Profile in Region 1 of Figure 2.

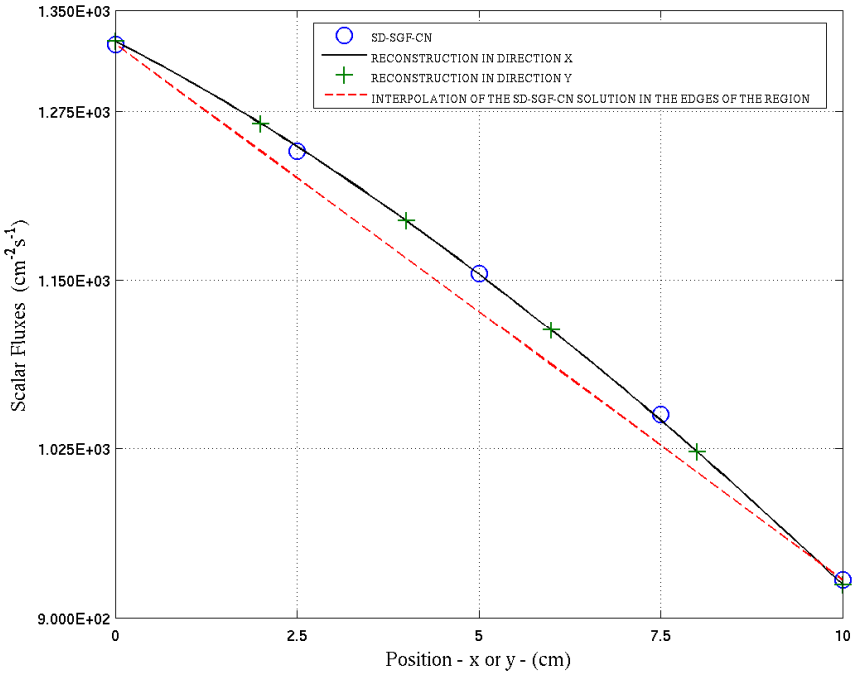

Figure 4. Scalar Flux Profile in Region 2 of Figure 2.

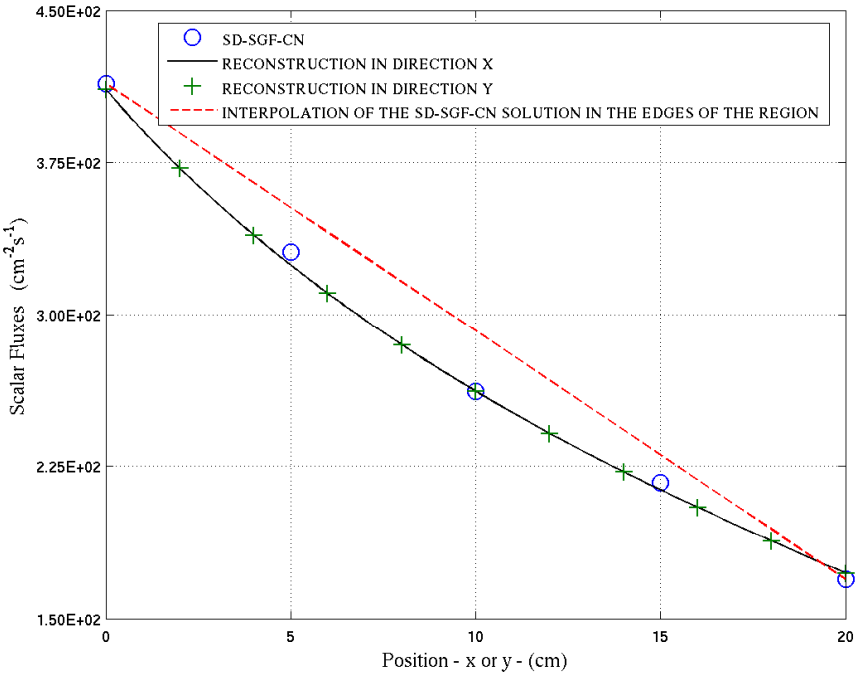

Figure 5. Scalar Flux Profile in Region 3 of Figure 2.

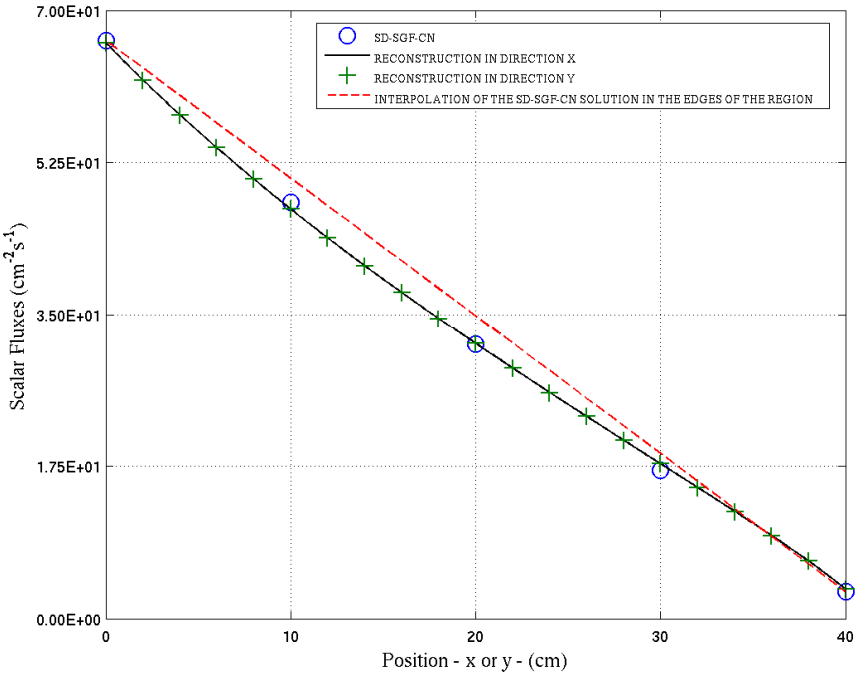

Figure 6. Scalar Flux Profile in Region 4 of Figure 2.

4. CONCLUSIONS

In this paper, the spectral nodal SD-SGF-CN method is used to determine the node-edge average angular fluxes along the edges of the discretization nodes with isotropic scattering in two-dimensional S_N eigenvalue problems.

The results presented in Table 2 and in Figure 3, 4, 5 and 6 indicate that we can use the analytical solutions of the S_N transverse-integrated nodal equations to perform the within-node reconstruction scheme of the node-edge average scalar flux. In general, the reconstruction scheme provides satisfactory results for the profile of the node-edge average scalar flux, with relative deviations that do not exceed 10% with respect to the SD-SGF-CN numerical results as generated on finer spatial grids. This is due to the fact that the SD-SGF-CN method is not free from spatial truncation error, as it is in slab geometry.

ACKNOWLEDGMENTS

The authors acknowledge the help given by Professor Gustavo M. Platt during the implementation of the reconstruction scheme as described in this paper. The authors also acknowledge Fundação Carlos Chagas Filho de Amparo à Pesquisa do Estado do Rio de Janeiro (FAPERJ – Brazil) for the financial support.

REFERENCES

1. BOLTZMANN, L. Weiture Studienubrt fsd Wormegleichgewicht unter. Gas-molekulen, Sitzungsber. Akad. Wiss. Wein, 66, 275-370, 1872..
2. CARLSON, B. G.; LATHROP, K. D. Transport theory - the method of discrete ordinates. In: GREENSPAN, H.; KELBER, C. N.; OKRENT, D. (Eds.). *Computing methods in reactor physics*. New York: Gordon and Breach, 1968. Cap. 3.
3. CHANDRASEKHAR, S. *Radiative transfer*. New York: Dover, 1960.
4. WICK, G. C. über ebene Diffusionsprobleme. *Zeitschrift für Physik*, v. 121, issue 11-12, p. 702-718, 1943.
5. LEWIS, E. E.; MILLER, W. F. *Computational methods of neutron transport.* Illinois: American Nuclear Society, 1993.
6. BURDEN, R. L.; FAIRES, J. D. *Numerical analysis*. 8th. ed. New York: Dover, 1993.
7. BADRUZZAMAN, A. Nodal methods in transport theory. *Advances in Nuclear Science and Technology*, v. 21, p. 293-331, 1990.
8. LAWRENCE, R. D.; DORNING, J. J. A discrete nodal integral transport theory for multidimensional reactor physics and shielding calculations. In: AMERICAN NUCLEAR SOCIETY TOPICAL MEETING. *Proceedings*… [S.l.]: Sun Valley, Idaho, USA, 1980.
9. ABREU, M. P.; BARROS, R. C. de. Um esquema para reconstrução analítica da solução dominante de problemas de autovalor unidimensionais multigrupo na formulação de ordenadas discretas. In: CONGRESSO NACIONAL DE MATEMÁTICA APLICADA E COMPUTACIONAL, 17.,1994, Vitória. *Anais*… Vitória: Sociedade Brasileira de matemática Aplicada e Computacional, 1994. p. 256-260.
10. MENEZES, W. A. Reconstrução intranodal da solução numérica gerada pelo método espectronodal constante para problemas S_N de autovalor em geometria retangular bidimensional. Dissertação (Mestrado) - Instituto Politécnico, Universidade do Estado de Rio de Janeiro, Nova Friburgo, 2009.
11. BARROS, R. C. ; LARSEN, E. W. . A Spectral Nodal Method for Discrete Ordinates Problems in X,Y-Geometry. In: ANS INTERNATIONAL TOPICAL MEETING; Advances in Mathematics, Computations and Reactor Physics, 1991, Pittsburgh. Proceedings. PITTSBURG-PA - EUA : American Nuclear Society, 1991. v. 2. p. 1-12.
12. ALVES, H. *Um método espectro nodal para problemas de autovalor na teoria de transporte de nêutrons segundo a formulação de ordenadas discretas*. 1999. Tese (Doutorado) - Instituto Alberto Luiz Coimbra de Pós-Graduação e Pesquisa, Universidade Federal do Rio de Janeiro, Rio de Janeiro, 1999.